Int. J. Solids Structures Vol. 22, No. 8, pp. 901–908, 1986
Printed in Great Britain.

0020-7683/86 $3.00 + .00
Pergamon Journals Ltd.

INVERSE PROBLEMS FOR ELASTIC PLATES WITH VARIABLE FLEXURAL RIGIDITY

C. H. QIU
Institute of Engineering Mechanics, Dalian Institute of Technology, Dalian, 116024, People's Republic of China

and

Y. M. CHEN
Department of Applied Mathematics and Statistics, State University of New York at Stony Brook, Stony Brook, NY 11794, U.S.A.

(*Received* 13 *February* 1984; *in revised form* 28 *February* 1985)

Abstract—The pulse-spectrum technique (PST), an iterative numerical algorithm, is extended and further developed to solve inverse problems in the dynamic structural identification and the dynamic structural design based on the two-dimensional elastic plate model with variable flexural rigidity. Numerical simulations on several simple examples are carried out to test the feasibility and to study the general characteristics of PST without the real measurement data for the case of dynamic structural identification or with the prescribed design data for the case of dynamic structural design. It is found that PST does give satisfactory results and also fares very well in regard to the given four practical criteria for evaluating numerical methods.

INTRODUCTION

Inverse problems in applied mechanics have attracted the attention of many engineers and scientists because of their importance in the structural identification and the structural design. Those of particular interest to us are the ones with measurement and design data being measured and prescribed, respectively, as functions of time, the dynamic structural identification and the dynamic structural design. The basic difference between the structural identification and the structural design problems depends on whether the data required for solving these inverse problems are measured or prescribed, respectively. In general, problems of this type can be formulated as ill-posed inverse problems of partial differential equations in the mathematical analysis; usually the solution of an inverse problem is not unique and does not depend continuously on the given data. Nevertheless, many numerical methods for solving problems of this type have been developed[1–6] and applied with success. Most of these techniques are based on the data from the measuring instruments placed at many different locations in the structure and on those known algorithms in the constrained optimization procedures; an exception is the pulse-spectrum technique (PST)[6] based on the idea that data are measured or prescribed at only very few locations on the surface of the structure in the time domain and the identification or design is carried out numerically in the complex frequency domain by a special iterative algorithm.

PST has been proven to be very successful also in solving many other kinds of inverse problems[7–15], and it has been shown that PST fares very well in regard to the following four practical criteria for the evaluation of any numerical method:

(1) *Universality criterion.* Whether or not a numerical method which is effective in one-space-dimensional problems can be extended with similar success into higher space-dimensional applications? Whether or not a solution method which is effective for solving inverse problems of one type of equations, e.g. hyperbolic or parabolic, can be extended to solve the inverse problems of the other type of partial differential equation with similar success and minimum effort?

(2) *Economy of data acquisition criterion.* The numerical method should be able to keep the difficulties and the cost expenditure of acquiring or measuring the necessary data for a successful calculation to a minimum.

(3) *Economy of programming effort criterion.* The numerical method should be as close to the nondedicated program as possible, because existing practices of programming new

dedicated numerical methods for all types of special problems can be unacceptably costly in many practical circumstances. Furthermore, the computer code should also contain as many as possible of the modules where the canned subroutines can readily be called upon.

(4) *Economy of computing cost criterion.* The numerical method should keep the cost of I/O and CPU times and the memory storage to a minimum.

In this paper, the PST is extended and further developed to solve problems in the dynamic structural identification and the dynamic structural design based on the two-dimensional elastic plate model. Numerical simulation on several simple examples are carried out to test the feasibility and to study the general characteristics of this numerical technique without the real measurement data (for the dynamic structural identification). It is found that PST does give excellent results.

PULSE-SPECTRUM TECHNIQUE (PST)

The partial differential equation for the deflection $W(x, y, t)$ of a vibrating two-dimensional elastic plate of homogeneous material is given by

$$\begin{aligned} &D(x,y)\,(\partial^4 W/\partial x^4+2\partial^4 W/\partial x^2\partial y^2+\partial^4 W/\partial y^4)+2\partial D(x,y)/\partial x\cdot(\partial^3 W/\partial x^3+\partial^3 W/\partial x\partial y^2)\\ &\quad+2\partial D(x,y)/\partial y\cdot(\partial^3 W/\partial y^3+\partial^3 W/\partial y\partial x^2)+2(1-\nu)\partial^2 D(x,y)/\partial x\partial y\cdot\partial^2 W/\partial x\partial y\\ &\quad+\partial^2 D(x,y)/\partial x^2(\partial^2 W/\partial x^2+\nu\partial^2 W/\partial y^2)+\partial^2 D(x,y)/\partial y^2(\partial^2 W/\partial y^2+\nu\partial^2 W/\partial x^2)\\ &\quad+\rho h(x,y)\partial^2 W/\partial t^2=0, \qquad (x,y)\in\Omega, \qquad 0<t<\infty, \end{aligned} \tag{1}$$

$$W(x,y,0)=\partial W(x,y,0)/\partial t=0, \qquad (x,y)\in\Omega, \tag{2}$$

and

$$B_k(W)|_{\Gamma_k}=F_k(x,y,t)|_{\Gamma_k}, \qquad k=1,2,3,\cdots,K, \tag{3}$$

where Ω is a bounded region in x–y space, $\Gamma=\Gamma_1+\Gamma_2+\cdots+\Gamma_K$ is the boundary of Ω, B_k is the boundary operator representing the corresponding boundary condition, ρ is the density, ν is the Poisson's ratio, E is the Young's modulus, $h(x,y)$ is the thickness of the plate and the flexural rigidity $D(x,y)$ is given by

$$D(x,y)=Eh^3(x,y)/12(1-\nu^2). \tag{4}$$

The inverse problem here is to determine the unknown coefficient $D(x,y)$ from the known coefficients ρ, ν and E, the known boundary functions $F_k(x,y,t)$, $k=1,2,3,\cdots,K$, and the additionally measured auxiliary data or the prescribed design requirements,

$$W(x,y,t)|_{\Gamma^*}=W^*(x,y,t), \qquad (x,y)\in\Gamma^*, \tag{5}$$

where Γ^* is a portion of Γ, and (5) is independent of (3).

Assuming that $W(x,y,t)$, $W^*(x,y,t)$ and $F_k(x,y,t)$, $k=1,2,3,\cdots,K$, are Laplace transformable, the PST calls for the Laplace transformation of (1)–(3) and (5) so that the entire system is transformed from the time domain to the complex frequency domain as

$$\begin{aligned} &D(x,y)\,(\partial^4 w/\partial x^4+2\partial^4 w/\partial x^2\partial y^2+\partial^4 w/\partial y^4)+2\partial D(x,y)/\partial x(\partial^3 w/\partial x^3+\partial^3 w/\partial x\partial y^2)\\ &\quad+2\partial D(x,y)/\partial y(\partial^3 w/\partial y^3+\partial^3 w/\partial y\partial x^2)+2(1-\nu)\partial^2 D(x,y)/\partial x\partial y\cdot\partial^2 w/\partial x\partial y\\ &\quad+\partial^2 D(x,y)/\partial x^2(\partial^2 w/\partial x^2+\nu\partial^2 w/\partial y^2)+\partial^2 D(x,y)/\partial y^2(\partial^2 w/\partial y^2+\nu\partial^2 w/\partial x^2)\\ &\quad+\rho h(x,y)s^2 w=0, \qquad (x,y)\in\Omega, \end{aligned} \tag{6}$$

$$B_k(w)|_{\Gamma_k}=f_k(x,y,s)|_{\Gamma_k}, \qquad k=1,2,3,\cdots,K, \tag{7}$$

and

$$w(x,y,s)|_{\Gamma^*} = w^*(x,y,s), \qquad (x,y)\in\Gamma^*, \tag{8}$$

where $w(x,y,s)$, $w^*(x,y,s)$ and $f_k(x,y,s)$, $k=1,2,3,\cdots,K$, are the Laplace transform of $W(x,y,t)$, $W^*(x,y,t)$ and $F_k(x,y,t)$, respectively. Now, the inverse problem becomes the determination of $D(x,y)$ from ρ, ν, E, $f_k(x,y,s)$, $k=1,2,3,\cdots,K$ and $w^*(x,y,s)$.

The iterative numerical algorithm begins by letting

$$w_{n+1} = w_n+\delta w_n, \qquad D_{n+1} = D_n+\delta D_n, \qquad n=0,1,2,3,\cdots, \tag{9}$$

where $D_0(x,y)$ is the initial guess of the unknown coefficient $D(x,y)$, $|\delta D_n| < |D_n|$ and $|\delta w_n| < |w_n|$. Upon substituting (9) into (6) and (7) and neglecting terms of order δ^2 and higher, one obtains an elliptic boundary value problem for w_n,

$$\begin{aligned} &D_n(\partial^4 w_n/\partial x^4+2\partial^4 w_n/\partial x\partial y^2+\partial^4 w_n/\partial y^4)+2\partial D_n/\partial x(\partial^3 w_n/\partial x^3+\partial^3 w_n/\partial x\partial y^2)\\ &\quad+2\partial D_n/\partial y(\partial^3 w_n/\partial y^3+\partial^3 w_n/\partial y\partial x^2)+2(1-\nu)\partial^2 D_n/\partial x\partial y\cdot\partial^2 w_n/\partial x\partial y\\ &\quad+\partial^2 D_n/\partial x^2(\partial^2 w_n/\partial x^2+\nu\partial^2 w_n/\partial y^2)+\partial^2 D_n/\partial y^2(\partial^2 w_n/\partial y^2+\nu\partial^2 w_n/\partial x^2)\\ &\quad+\rho s^2\{12(1-\nu^2)/E\}^{1/3}D_n^{1/3}w_n = 0, \qquad (x,y)\in\Omega, \end{aligned} \tag{10}$$

$$B_k(w_n)|_{\Gamma_k} = f_k(x,y,s), \qquad k=1,2,3,\cdots,K, \tag{11}$$

and another elliptic boundary value problem for δw_n,

$$\begin{aligned} &D_n(\partial^4\delta w_n/\partial x^4+2\partial^4\delta w_n/\partial x^2\partial y^2+\partial^4\delta w_n/\partial y^4)+2\partial D_n/\partial x(\partial^3\delta w_n/\partial x^3+\partial^3\delta w_n/\partial x\partial y^2)\\ &\quad+2\partial D_n/\partial y(\partial^3\delta w_n/\partial y^3+\partial^3\delta w_n/\partial y\partial x^2)+2(1-\nu)\partial^2 D_n/\partial x\partial y\cdot\partial^2\delta w_n/\partial x\partial y\\ &\quad+\partial^2 D_n/\partial x^2(\partial^2\delta w_n/\partial x^2+\nu\partial^2\delta w_n/\partial y^2)+\partial^2 D_n/\partial y^2(\partial^2\delta w_n/\partial y^2+\nu\partial^2\delta w_n/\partial x^2)\\ &\quad+\rho s^2\{12(1-\nu^2)/E\}^{1/3}D_n^{1/3}\delta w_n = -\delta D_n(\partial^4 w_n/\partial x^4+2\partial^4 w_n/\partial x^2\partial y^2+\partial^4 w_n/\partial y^4)\\ &\quad-2\partial\delta D_n/\partial x(\partial^3 w_n/\partial x^3+\partial^3 w_n/\partial x\partial y^2)-2\partial\delta D_n/\partial y(\partial^3 w_n/\partial y^3+\partial^3 w_n/\partial y\partial x^2)\\ &\quad-2(1-\nu)\partial^2\delta D_n/\partial x\partial y\cdot\partial^2 w_n/\partial x\partial y-2\partial^2\delta D_n/\partial x^2(\partial^2 w_n/\partial x^2+\nu\partial^2 w_n/\partial y^2)\\ &\quad-\partial^2\delta D_n/\partial y^2(\partial^2 w_n/\partial y^2+\nu\partial w_n/\partial x^2)\\ &\quad-3^{-1}\delta D_n\rho s^2\{12(1-\nu^2)/E\}^{1/3}D_n^{-2/3}w_n, \qquad (x,y)\in\Omega, \end{aligned} \tag{12}$$

$$B_k(\delta w_n)|_{\Gamma_k} = 0, \qquad k=1,2,3,\cdots,K. \tag{13}$$

By using the method of Green's function, the boundary value problem of (12) and (13) can be changed to a Fredholm integral equation of the first kind which relates $\delta D_n(x,y)$ to $\delta w_n(x,y,s)$ as

$$\begin{aligned} &\int\!\!\int_\Omega G_n(x,y;x',y',s)\{\delta D_n(\partial^4 w_n/\partial x'^4+2\partial^4 w_n/\partial x'^2\partial y'^2+\partial^4 w_n/\partial y'^4)\\ &\quad+2\partial\delta D_n/\partial x'(\partial^3 w_n/\partial x'^3+\partial^3 w_n/\partial x'\partial y'^2)+2\partial\delta D_n/\partial y'(\partial^3 w_n/\partial y'^3+\partial^3 w_n/\partial y'\partial x'^2)\\ &\quad+2(1-\nu)\partial^2\delta D_n/\partial y'\partial x'\cdot\partial^2 w_n/\partial x'\partial y'+\partial^2\delta D_n/\partial x'^2(\partial^2 w_n/\partial x'^2+\nu\partial^2 w_n/\partial y'^2)\\ &\quad+\partial^2\delta D_n/\partial y'^2(\partial^2 w_n/\partial y'^2+\nu\partial^2 w_n/\partial x'^2)+3^{-1}\delta D_n\rho s^2\{12(1-\nu^2)/E\}^{1/3}D_n^{-2/3}w_n\}\,dx'\,dy'\\ &= -\delta w_n(x,y,s), \end{aligned} \tag{14}$$

where $G_n(x,y;x',y',s)$ is the Green's function of (12) and (13) and it can be computed numerically in general.

For the purpose of accelerating the rate of convergence, the right-hand side of (14) can be replaced by $w_n(x, y, s) - w(x, y, s)$. After setting (x, y) on Γ^* and using (8), from (14) one obtains the following Fredholm integral equation of the first kind of $\delta D_n(x, y)$,

$$\int\int_{\Omega} G_n|_{\Gamma^*}\{\delta D_n(\partial^4 w_n/\partial x'^4 + 2\partial^4 w_n/\partial x'^2\partial y'^2 + \partial^4 w_n/\partial y'^4) + 2(1-\nu)\partial^2\delta D_n/\partial x'\partial y' \cdot \partial^2 w_n/\partial x'\partial y'$$
$$+ 2\partial\delta D_n/\partial x'(\partial^3 w_n/\partial x'^3 + \partial^3 w_n/\partial x'\partial y'^2) + 2\partial\delta D_n/\partial y'(\partial^3 w_n/\partial y'^3 + \partial^3 w_n/\partial y'\partial x'^2)$$
$$+ \partial^2\delta D_n/\partial x'^2(\partial^2 w_n/\partial x'^2 + \nu\partial^2 w_n/\partial y'^2) + \partial^2\delta D_n/\partial y'^2(\partial^2 w_n/\partial y'^2 + \nu\partial^2 w_n/\partial x'^2)$$
$$+ 3^{-1}\delta D_n \rho s^2\{12(1-\nu^2)/E\}^{1/3} D_n^{-2/3} w_n\}\, dx'\, dy' = w_n(x, y, s)|_{\Gamma^*} - w^*(x, y, s)|_{\Gamma^*}. \tag{15}$$

Equations (9), (10), (11) and (15) form the basic structure for each iteration in the iterative numerical algorithm of PST. First, a numerical integration subroutine is used to evaluate the Laplace transforms $f_k(x, y, s)$, $k = 1, 2, 3, \cdots, K$ and $w^*(x, y, s)$ and $s = s_i$, $i = 1, 2, 3, \cdots, I$. Then these discrete values will be used to solve (10), (11) and (15) numerically. Boundary value problem (10) and (11) and the Green's function of (12) and (13) can be solved numerically by using the standard finite element method and here a finite element elliptic solver developed at Dalian Institute of Technology is used to solve (10) and (11) and for the Green's function of (12) and (13) I-times for different s_i's. The Fredholm integral equation of the first kind (15) can be discretized by simply using the trapezoid rule with the derivatives of the functions of the integrand being approximated by the same formulae in the finite element method. Hence (15) can be reduced to a linear algebraic system,

$$\mathbf{M}_n(w_n, G_n, s_i) \cdot \delta\mathbf{D}_n(x_j, y_m) = \mathbf{R}_n(s_i), \tag{16}$$

where the known matrix $\mathbf{M}_n(w_n, G_n, s_i)$ comes from the discretization of the integral with each row containing a different s_i, the known vector $\mathbf{R}_n(s_i)$ comes from the discretization of the right-hand side of (15) with each component depending on its corresponding complex frequency s_i, and the unknown vector $\delta\mathbf{D}_n(x_j, y_m)$ consists of all $\delta D_n(x_j, y_m)$. Since $\mathbf{M}_n$ is either a rectangular matrix or an ill-conditioned square matrix, Tikhonov's regulation method[16] is used to solve it.

It is important to notice that each cycle of iteration consists essentially of first solving the direct boundary value problem (10) and (11) and the Green's function of (12) and (13) I-times and then solving the Fredholm integral equation of the first kind (15) once.

NUMERICAL SIMULATION

In order to test the feasibility and to study the general characteristics of the PST computational algorithm for solving the inverse problems of elastic plates with variable flexural rigidity, the following numerical simulation procedure is carried out:

First one chooses a $D^*(x, y)$ which is supposed to represent the correct flexural rigidity and also the boundary conditions $F_k(x, y, t)$, $k = 1, 2, 3, \cdots, K$, which are supposed to represent the measured data on applied disturbances or the required design data. After their Laplace transforms $f_k(x, y, s)$, $k = 1, 2, 3, \cdots, K$, are numerically computed for a discrete set of $s = s_i$, $i = 1, 2, 3, \cdots, I$, the elliptic boundary value problem (6) and (7) with the chosen $D^*(x, y)$ and $f_k(x, y, s_i)$, $k = 1, 2, 3, \cdots, K$, are solved I-times for different s_i's by using the finite element method; thus one generates the rest of the supposedly measured data or required design data $w^*(x, y, s_i)$, $i = 1, 2, 3, \cdots, I$.

Next, $D_0(x, y)$ is assumed. Hence upon solving (9)–(11) and (15) numerically, $D_1(x, y)$ is obtained. Then in a similar manner $D_2(x, y)$ is obtained. One continues this procedure until finally a numerical limit $D_N(x, y)$ is reached. Other than the truncation, round-off, numerical integration and finite element approximation errors in both generating the numerical data and computing $D_N(x, y)$, any norm (e.g. maximum norm, L_2 norm) of $D^*(x, y) - D_N(x, y)$ can be used as a criterion for evaluating the performance of the com-

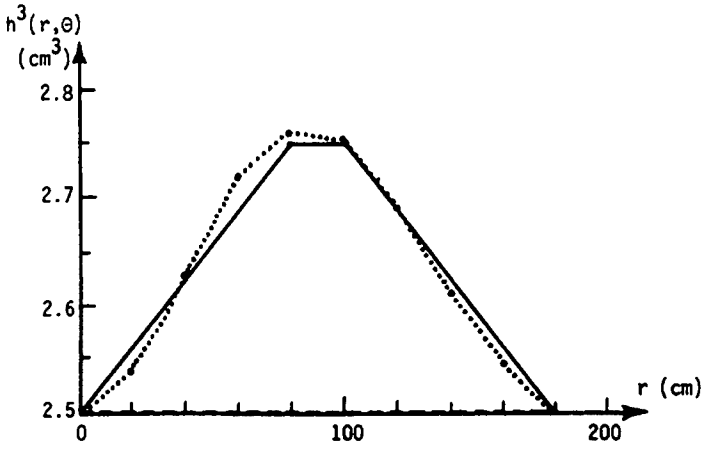

Fig. 1. Comparison of the calculated $h_N^3(r,\theta)$ (dotted line) and the exact $h^{3*}(r,\theta)$ (solid line), with the initial guess $h_0^3(r,\theta)$ (dashed line) for a symmetric circular plate.

putational algorithm of PST. In particular, it should be pointed out that the numerically generated auxiliary data $w^*(x,y,s_i)$, $i=1,2,3,\cdots,I$, are not error free; especially, errors are quite large when a coarse computational grid is used, because they are of $O\{(\Delta x/L)^2\}$, where Δx is a typical distance between two neighboring grid points, and L is a typical dimension of Ω. Due to the uncontrollable nature of these errors, one can consider them to be equivalent to the noise in the measured data. Furthermore, one can introduce additional artificial noise by adding to the input data any numbers generated by a random number generator.

For pure economic reasons, coarse computational grids are used in the numerical simulations here. First, two examples are symmetric circular plates with a variable flexural rigidity as a function of radial variable r only. They are simply supported on the edge $r=a$; hence the corresponding boundary conditions are $W(a,\theta,t)=\partial^2 W(a,\theta,t)/\partial r^2+(\nu a^{-1})\partial W(a,\theta,t)/\partial r=0$. For simplicity, a cosine pulse, $W(0,\theta,t)=\cos(\pi/2)t$, $0\leqslant t\leqslant 1$ sec, $W(0,\theta,t)=0$, 1 sec $\leqslant t<\infty$, is applied at the center of the circular plate, and the auxiliary data $W^*(r,\theta,t)$ is also measured at the center of the plate. Moreover, $E=20$ Tg/m^2, $\nu=0.3$ and $\rho=7.8$ Mg/m^3 are used, and then the only unknown parameter is the thickness of the plate $h(r,\theta)=h(r)$, Here $s_i=(0.2)^{1/2}$, $(0.4)^{1/2}$, $(0.6)^{1/2}$, $(0.8)^{1/2}$, 1, $(1.2)^{1/2}$, $(1.4)^{1/2}$, $(1.6)^{1/2}$, $(1.8)^{1/2}$, 2 sec^{-1}, $a=1.8$ m and $\Delta r=0.2$ m are used in our computation. The numerical results coverage after eight iterations and they are plotted in Figs. 1 and 2. The estimated CPU time is 38 sec for each example on the UNIVAC 1100 at SUNY at Stony

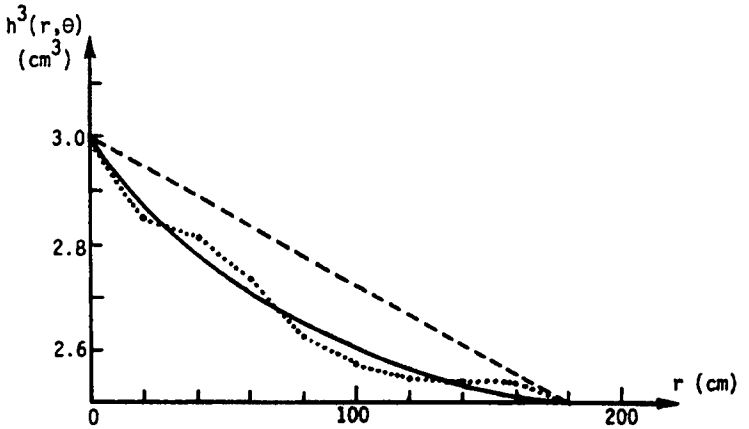

Fig. 2. Comparison of the calculated $h_N^3(r,\theta)$ (dotted line) and the exact $h^{3*}(r,\theta)$ (solid line), with the initial guess $h_0^3(r,\theta)$ (dashed line) for a symmetric circular plate.

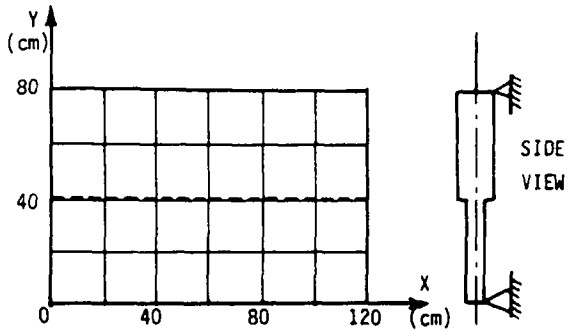

Fig. 3. The top and side views of a rectangular plate and the computational grid system.

Brook. The third example is a simply supported rectangular plate with a discontinuous flexural rigidity in one direction (Fig. 3). It has the same material parameters as the first two examples; the same cosine pulse is applied at the center of the rectangular plate and the auxiliary data is also measured at the center of the plate. However, here $s_i = 1, (2)^{1/2}, (3)^{1/2}, 2, (5)^{1/2}, (6)^{1/2}, (7)^{1/2}, (8)^{1/2}, 3, (10)^{1/2}\,\text{sec}^{-1}$. The numerical results converge after seven iterations with 9-sec CPU time, and they are plotted in Fig. 4. The last example is to determine $h^{(2)}(x, y)/h^{(1)}(x, y)$ of a simply supported square plate with discontinuous thickness (Fig. 5). The material parameters, applied loading and data measurement are the same as

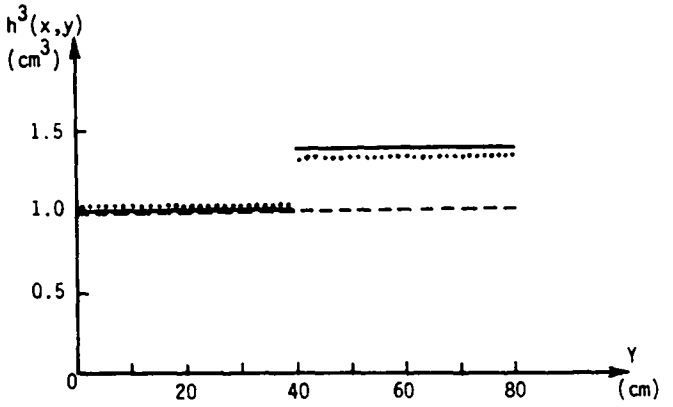

Fig. 4. Comparison of the calculated $h_N^3(x, y)$ (dotted line) and the exact $h^{3*}(x, y)$ (solid line), with the initial guess $h_0^3(x, y)$ (dashed line) for the rectangular plate in Fig. 3.

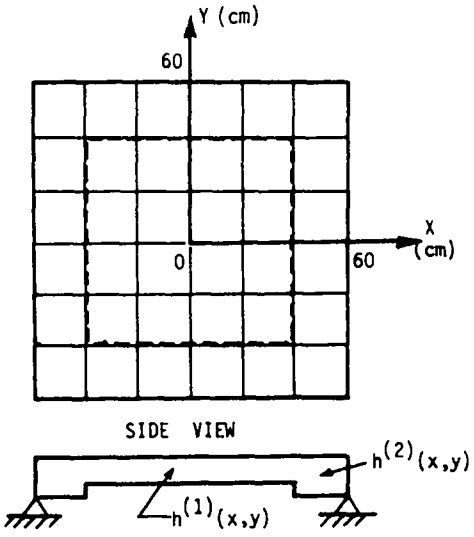

Fig. 5. The top and side views of a square plate and the computational grid system.

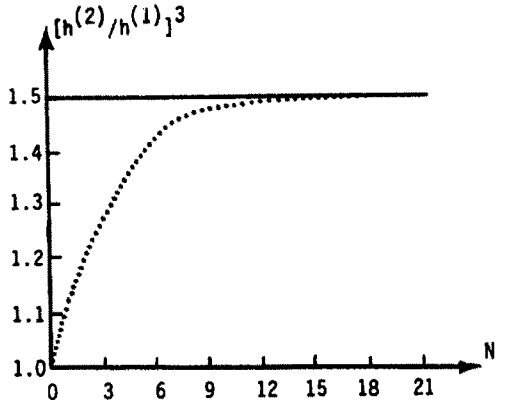

Fig. 6. Comparison of the calculated $\{h^{(2)}/h^{(1)}\}_N^3$ (dotted line) and the exact $\{h^{(2)}/h^{(1)}\}^{3*}$ (solid line) as a function of N, number of iteration, for the square plate in Fig. 5.

the previous three examples, and the complex frequency selection is the same as the third example. 12-sec CPU time is needed to perform eighteen iterations, and the numerical results are plotted in Fig. 6.

DISCUSSION

The results of numerical simulation have demonstrated that, even with coarse grid systems, the PST iterative numerical algorithm does give very good results in the dynamic structural identification and the dynamic structural design. Its accuracy can be greatly improved if a finer grid system and a larger number of s_i's are used. The relevant data are given in the following Table 1, where Δx is a typical distance between two neighboring grid points, and L is a typical dimension of Ω. These data are well within the ranges of the performance indexes of PST established previously by performing numerical simulations on several hundred different examples.

There is no practical method to determine *a priori* the proper values of s_i, $i = 1, 2, 3, \cdots, I$, or their optimum values if they do exist. However, from our past experiences, the PST is not sensitive to the precise values of s_i but to the range of s_i as long as they are not too close to each other. As the rule of thumb, the values of s_i should not be too large and we have found that the range $0 < s_i < 100$ is very good; otherwise, when s_i, $i = 1, 2, 3, \cdots, I$, are too large, the elliptic boundary value problem (10) and (11) becomes too stiff and hard to be solved accurately. Some examples have been solved with different sets of s_i, $i = 1, 2, 3, \cdots, I$, but in the same range; it is found that the maximum pointwise deviations are less than 5%.

Efforts in applying PST to multiparameter $\{E(x, y)$, $\nu(x, y)$, $\rho(x, y)$, $h(x, y)$, $\eta(x, y)$ (damping coefficient)$\}$ inverse problems of the plate equation are underway. We are confident that this endeavor will be quite successful, because it has been demonstrated that

Table 1

Example	$\Delta x/L$	α Regularization parameter	CPU time (sec)	No. of iterations	$\frac{\text{Max}\lvert h^{3*}-h_0^3\rvert(x,y)}{\text{Max}\lvert h^{3*}\rvert(x,y)}$	$\frac{\text{Max}\lvert h^{3*}-h_N^3\rvert(x,y)}{\text{Max}\lvert h^{3*}\rvert(x,y)}$	$\frac{\text{Max}\lvert h^{3*}-h_N^3\rvert(x,y)}{\text{Max}\lvert h^{3*}-h_0^3\rvert(x,y)}$
1	0.11	10^{-5}	38	8	0.091	0.011	0.121
2	0.11	10^{-4}	38	8	0.041	0.011	0.268
3	0.17	5×10^{-5}	9	7	0.249	0.020	0.080
						Here h^3 is replaced by $\{h^{(2)}/h^{(1)}\}^3$	
4	0.17	10^{-4}	6	9	0.333	0.013	0.039

PST is capable of solving multiparameter inverse problems of the acoustic wave equation[13] and the elastic wave equation[15]. Their results will be reported elsewhere in the future.

REFERENCES

1. N. Distefeno and A. Ruth, System identification in nonlinear structural seismic dynamics. *Comput. Math. Appl. Mech. Engng* 353–372 (1975).
2. F. E. Udwadia and P. C. Shah, Identification of structures through records obtained during strong earthquake ground motion. *J. Engng Ind., Trans. ASME* 1347–1362 (1976).
3. G. H. Hart and J. T. P. Yao, System identification in structural dynamics. *J. Engng Mech. Div., ASCE* 103(EM6) (1977).
4. S. S. Simonian, Inverse problems in structural dynamics–I. *Int. J. Numer. Methods Engng* **17**, 357–365 (1981).
5. S. S. Simonian, Inverse problems in structural dynamics–II. *Int. J. Numer. Methods Engng* **17**, 367–386 (1981).
6. Y. M. Chen and Y. Lin, An iterative algorithm for solving inverse problems in structural dynamics. *Int. J. Numer. Methods Engng* **19**, 825–829 (1983).
7. Y. M. Chen and D. S. Tsien, A numerical algorithm for remote sensing or density profiles of a simple ocean model by acoustic pulses. *J. Comput. Phys.* **25**, 366–385 (1977).
8. D. S. Tsien and Y. M. Chen, A pulse-spectrum technique for remote sensing of stratified media. *Radio Sci.* **13**, 775–783 (1978).
9. Y. M. Chen and J. Q. Liu, A numerical algorithm for remote sensing of thermal conductivity. *J. Comput. Phys.* **43**, 315–326 (1981).
10. Y. M. Chen and X. T. Weng, Computer-aided partial synthesis of lossless non-uniform lines of finite length. *Circuit Theory Appl.* **10**, 69–79 (1982).
11. R. P. Hatcher and Y. M. Chen, An iterative method for solving inverse problems of a nonlinear wave equation. *SIAM J. Sci. Stat. Comput.* **4**, 149–163 (1983).
12. Y. M. Chen and J. Q. Liu, A numerical algorithm for solving inverse problems of two-dimensional wave equations. *J. Comput. Phys.* **50**, 193–208 (1983).
13. Y. M. Chen and J. Q. Liu, An iterative numerical algorithm for solving multi-parameter inverse problems of evolutional partial differential equations. *J. Comput. Phys.* **53**, 429–442 (1984).
14. J. Q. Liu and Y. M. Chen, An iterative algorithm for solving inverse problems of two-dimensional diffusion equations. *SIAM J. Sci. Stat. Comput.* **5**, 255–269 (1984).
15. Y. M. Chen and G. Q. Xie, A numerical method for simultaneous determination of bulk modulus, shear modulus and density variations for nondestructive evaluation. *Nondestruct. Test. Commun.* **1**, 125–135 (1984).
16. A. N. Tikhonov and V. Y. Arsenin, *Solutions of Ill-Posed Problems*. Wiley, New York (1977).